Author's personal copy

Available online at www.sciencedirect.com
ScienceDirect
Acta Materialia 57 (2009) 2321–2327
Acta MATERIALIA
www.elsevier.com/locate/actamat

Effect of superimposed uniaxial stress on rumpling of platinum-modified nickel aluminide coatings

Sebastien Dryepondt, David R. Clarke *

Materials Department, College of Engineering, University of California, Santa Barbara, CA 93106-5050, USA

Received 17 June 2008; received in revised form 8 December 2008; accepted 30 January 2009
Available online 28 February 2009

Abstract

Thermal cycling of a platinum modified, nickel aluminide (Ni,Pt)Al coated single crystal superalloy, between 1000 and 1150 °C with 10 min holds at each temperature, and subject to a compressive uniaxial stress is reported. There are two major effects of the superimposed compressive stress not observed in the absence of the stress. One is that the rumpling pattern exhibits an asymmetry with an increase of the bond coat surface roughness perpendicular to the applied loading axis. The other is the formation of cracks in the thermally grown oxide aligned parallel to the stress axis.
© 2009 Acta Materialia Inc. Published by Elsevier Ltd. All rights reserved.

Keywords: Coating; Rumpling; Profilometry; Grain structure; Cyclic oxidation testing

1. Introduction

Platinum-modified nickel aluminide coatings are widely used in the gas turbine industry to protect superalloy components, such as vanes and blades, from oxidation and corrosion [1–3]. Like other coatings, the life of these coatings can degrade by a variety of phenomena associated with their exposure to high temperatures and thermal cycling. Among these, surface roughening can occur at temperatures above about 1100 °C, particularly under cyclic oxidation conditions [4]. The roughening phenomenon, often referred to as rumpling, is detrimental for a variety of reasons, ranging from increasing the heat transfer coefficient between the turbine gas flow and the coating to the initiation of local debonding and failure of thermal barrier ceramic top-coats deposited on top of the aluminide coatings.

Although a number of extensive studies have now been made of the rumpling phenomenon, none as far as we are aware has been performed with a superimposed stress. Our primary motivation for investigating the effect of a uniaxial stress, which we do in this work, was to ascertain whether the symmetry of rumpling is affected by an applied stress. It was also to determine whether stresses such as those that occur in rotating airfoils might influence rumpling. Although airfoils are subject to tensile centrifugal forces, flexural and torsional vibrations can introduce significant compressive and shear stresses. In addition, there is growing evidence that under isothermal strain controlled compression cyclic fatigue of coated superalloys, coatings deform in the tensile unloading phase of the fatigue cycle and crack [5]. This has been referred to as sustained peak, low cycle fatigue cracking (SPLIFC) [5,6].

For these reasons, the effect of a superimposed 80 MPa compressive stress on rumpling has been investigated in this work. This particular value of compressive stress was chosen after preliminary experiments had shown that it was sufficient to cause creep in the superalloy over the temperature range studied. Permanent deformation in the superalloy was considered necessary so as to better represent the range of strains over which the effect of an applied stress on rumpling might be pertinent to severe airfoil conditions. The samples were cycled over a narrow temperature range, between 1000 and 1150 °C, since earlier studies have shown that the rumpling principally occurs over this

* Corresponding author. Tel.: +1 805 893 8486.
E-mail address: clarke@engineerimg.ucsb.edu (D.R. Clarke).

1359-6454/$36.00 © 2009 Acta Materialia Inc. Published by Elsevier Ltd. All rights reserved.
doi:10.1016/j.actamat.2009.01.040

Author's personal copy

narrow temperature cycle [7]. This is also the temperature range over which the thermal expansion coefficient of the superalloy rapidly changes with temperature and is larger than that of nickel-aluminide [8]. For similar reasons, and to better represent the effect of short high temperature cycling that mimics certain high-performance aircraft missions, ten minute thermal cycles were used rather than the longer one-hour cycles often used in thermal cycling tests. Shorter thermal cycles have also been shown to lead to enhanced rumpling [4]. Together, it was anticipated that this combination of cyclic thermal–mechanical conditions would accelerate any effects of an applied compressive stress on rumpling behavior.

2. Experimental procedure

Compressive test specimens, rectangular parallelepiped in shape $10 \times 5 \times 3$ mm, were machined from one-inch diameter furnace cycle test (FCT) coupons of CMSX-4 single crystal superalloys coated with a standard Pt-modified diffusion aluminide. The specimens were machined so that the long direction was oriented parallel to the [001] axis of the superalloy, determined by etching and X-ray diffraction. This is the elastically "soft" direction of the superalloy. Prior to testing, the coating surface was first diamond and then SiC polished to remove the grain boundary regions formed during the aluminizing process. The samples were then annealed for 1 h at 1150 °C in a horizontal furnace with a heating rate close to 200 °C/min to avoid the formation of transient alumina during the initial ramp up to the lower cycle temperature. This pre-treatment ensured the rapid formation of a uniform, alpha alumina thermally grown oxide (TGO) over the bond-coat surface. Compressive testing was performed using an MTS hydraulic-machine, equipped with a high temperature resistance furnace and SiC compression rods. To protect the load cell and enhance the specimen cooling rate in the decreasing temperature portion of the thermal cycles so as to facilitate the short cycle times, the SiC rods were held in water cooled clamps. The temperature of the test specimen was monitored during testing with an R-type thermocouple welded onto the back side of the specimen and the temperature was used to adjust the furnace power. Concurrently, the cross-head displacement was monitored and the load adjusted to maintain a constant stress. The temperature was cycled between a 10 min dwell at 1150 °C followed by a 10 min dwell at 1000 or 400 °C. In every test, an identical specimen was placed on the top of the lower SiC rod, adjacent to the compression specimen, subjecting it to the same heat treatment but without any applied stress. This was used as a reference for the purposes of measuring the rumpling amplitude in the absence of a superimposed stress.

To ensure temperature homogeneity in the furnace before starting the cyclic tests, the ramping to the lower temperature of the cycle was carried out with a low heating rate. A constant 80 MPa compressive stress was then applied after the temperature of the specimen became stable and the temperature cycling was then begun. Two specimens tested for 60 cycles between 1150 and 1000 °C were interrupted after 20 and 40 cycles to follow the surface evolution with the number of cycles. One test was interrupted after 82 cycles because the onset of tertiary creep was observed.

The surface morphology of the samples before and after thermo-mechanical testing was quantified using a Wyco optical interferometer profiling system (NT1100). The interferometer data were converted into profile maps with the Vision software of the interferometer and Matlab software was used to carry out statistical analyses of the surface profiles.

3. Results

The variation in cross-head displacement and temperature is plotted in Fig. 1a for a specimen cycled 82 times between 1000 and 1150 °C. An expanded view of two of the cycles is shown in Fig. 1b. To maintain a constant

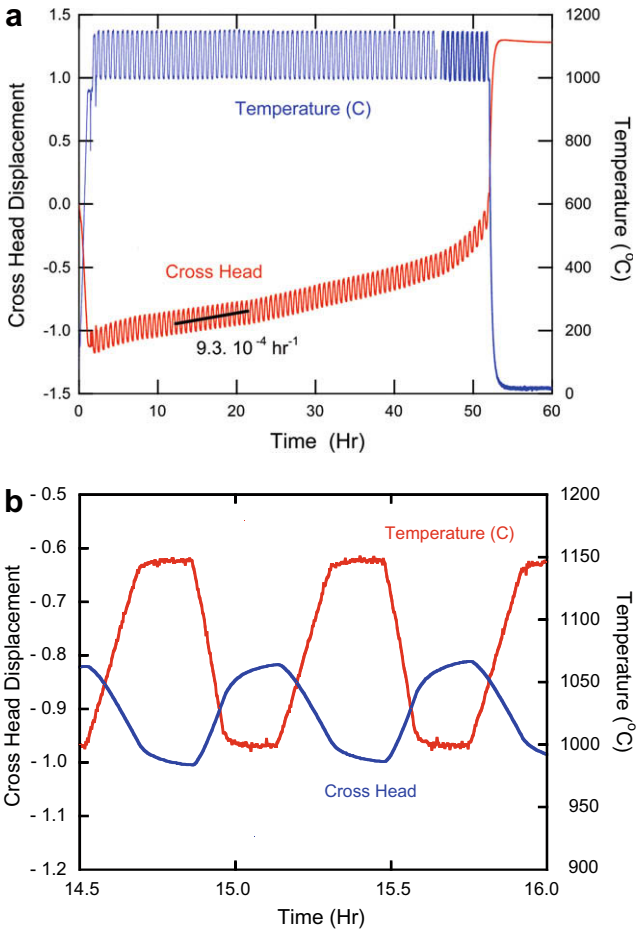

Fig. 1. Cross-head displacement and temperature variation during thermal cycling between 1150 and 1000 °C of a specimen subject to a 80 MPa compressive applied stress. (a) Complete test also showing the creep deformation of the specimen. (b) Enlargement of the test data to show in greater detail two consecutive cycles.

Author's personal copy

applied stress, the hydraulic actuator, located beneath the specimen, was used to balance the thermal expansion of the specimen and the SiC rods during thermal cycling. The thermal inertia of the SiC rods is, however, such that the cross-head position is still decreasing during the dwell at 1150 °C (Fig. 1b). As a result it was not possible to measure any instantaneous creep. Nevertheless, as can be seen in Fig. 1a, a progressive deformation of the specimen is observed after several cycles. The overall creep rate was measured to lie between 9.3×10^{-4} and $3.5 \times 10^{-4}\,h^{-1}$, values consistent with creep data found in the literature for the second-generation superalloys under cyclic conditions [9]. The test with the highest creep rate was interrupted after 82 cycles because of the onset of tertiary creep and thickening of the specimen towards one end.

Digital images of the surface of the sample tested for 82 cycles are presented in Fig. 2 together with a region of the same size on the accompanying reference sample subject to the same rapid thermal cycling. In contrast to observations of the reference thermally cycled samples the roughness varied with position over the sample surface. In addition, there was a marked anisotropy of the roughness variation from place to place but in each area examined the roughening was aligned perpendicular to the applied stress direction. The interferometer images in Fig. 2a–c are of different regions of the coating with the image in Fig. 2c

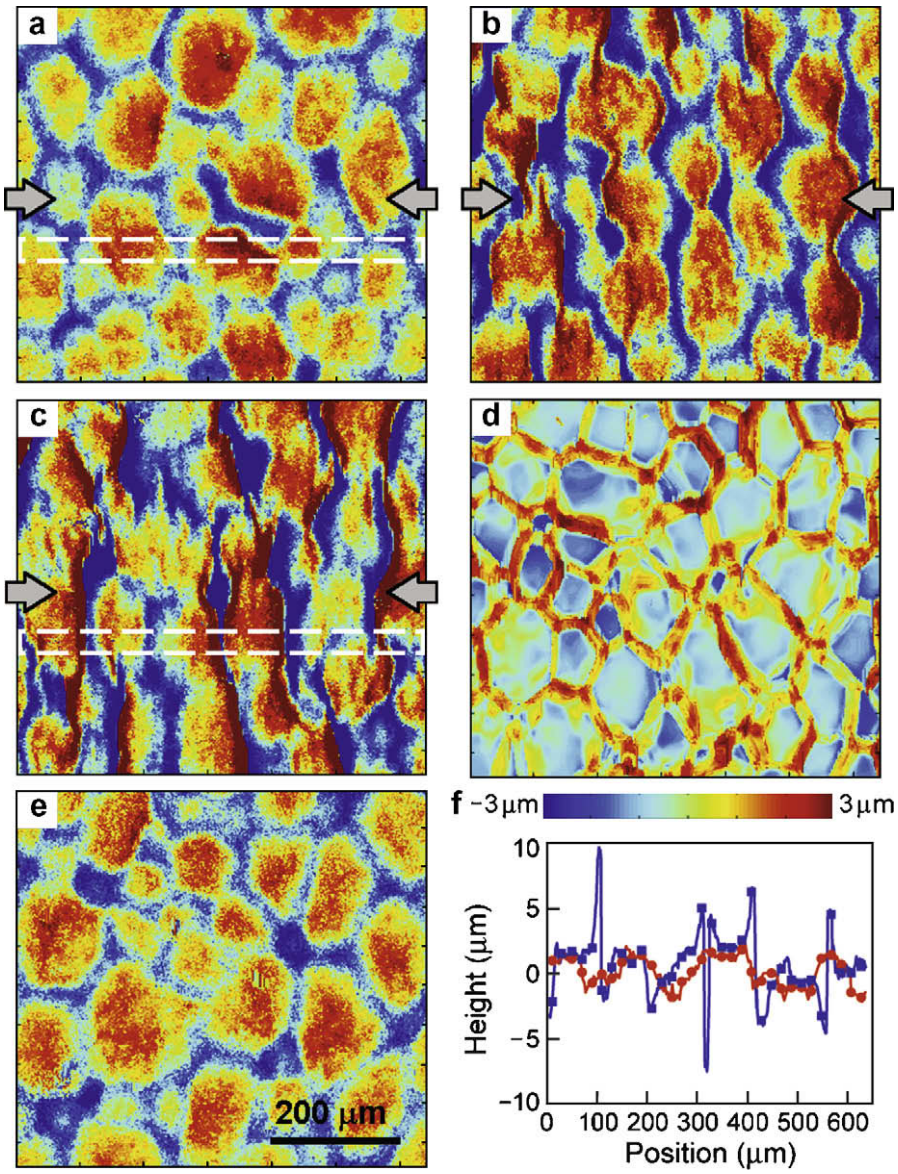

Fig. 2. Interferometry images of the specimen cycled 82 times between 1000 and 1150°C. The arrows indicate the applied stress direction. (a–c) Different regions on the surface of a specimen subject to 80 MPa compressive stress. (d) Is the identical region to that in (b) but before thermomechanical testing and polishing away the grain boundary ridges. The ridges produced by the aluminizing step facilitate identification of the individual grains and the corresponding height variations. (e) Reference specimen with no stress applied. (f) Average line scan profiles along the stress axis from the regions delineated by the dashed white lined box in (a) and (c).

Author's personal copy

closest to the one end of the sample where the distortions associated with tertiary creep where most marked. The image in Fig. 2d is of the identical area as of Fig. 2b but before testing and polishing away the grain boundary ridges formed during the aluminizing process. The surfaces of the majority of the grains appear with the same color indicating that they are at the same height with the higher ridges along the grain boundaries. Comparison of the images clearly indicates that individual grains have moved relative to one another to create the appearance of aligned features evident in the Fig. 2b. Also for comparison, Fig. 2e is an image of the reference sample: no alignment or preferential direction is evident in the height of individual grains.

The rumpling anisotropy was quantified from the digital images by determining the rumpling amplitude, R_q, from line scans parallel to the loading axis for R_q^x and perpendicular to the loading axis for R_q^y. The ratio of these two roughness values, R_q^x/R_q^y, is the roughness anisotropy shown in Fig. 3. The data for the average rumpling amplitude, R_q, on the abscissa was obtained from the identical images that the anisotropy ratio were determined. In compiling the data in Fig. 3, line scans parallel and perpendicular to the applied load direction were recorded at different locations on specimens cycled 60 times and 80 times between 1000 and 1150 °C. The notable feature of the data is that there is an approximately linear relationship between the anisotropy ratio and the rumpling amplitude. In contrast, when no stress was applied, although the roughness increases with the number of cycles, the anisotropy ratio R_q^x/R_q^y remains close to unity.

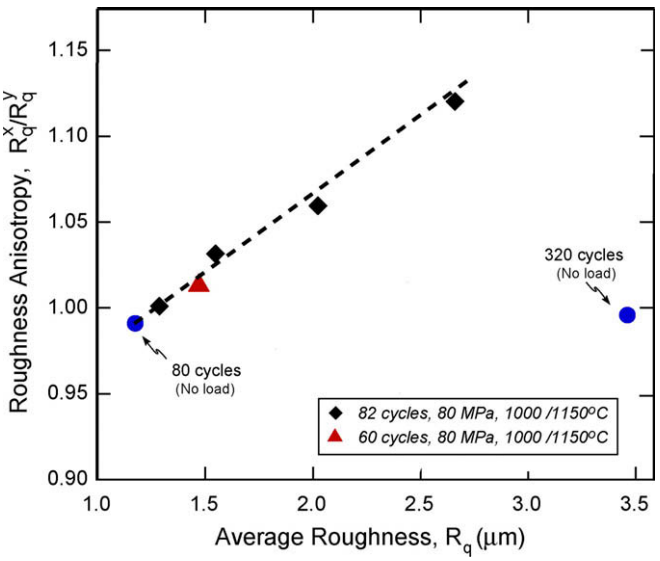

Fig. 3. The ratio of the roughness parallel and perpendicular to the applied stress direction, R_q^x/R_q^y, as a function of the RMS roughness, R_q, for specimens cycled between 1000 and 1150 °C. Results from a specimen cycled between room temperature and 1150 °C without any applied stress have been added as a reference. The dashed line through the data is a guide to the eye.

One of the other striking features of the height variation images is the abrupt changes in height in some locations. This is particularly evident in Fig. 2c. To emphasize this feature, the height variation, obtained by averaging 10 scan lines parallel to the loading axis from the images of Fig. 2b and c, are given in Fig. 2f. In addition to the height variations, that are mainly associated with individual grains in the aluminide, there are very abrupt changes in height that coincide with some of the grain boundaries lying perpendicular to the loading axis. It is noted that these variations in height are several times the rumpling heights elsewhere.

To elucidate the nature of the abrupt height variations detected by the interferometer, a series of optical and scanning electron micrographs were also recorded. Optical micrographs of cross-sections made along the load axis, such as Fig. 4a, indicate that there are sharp changes in the cross-section, several which occur in the vicinity of the grain boundaries in the aluminide. Scanning electron microscopy reveals that there are large changes in surface slope at these steps suggesting severe localization of the deformation of the aluminide. In every case, the TGO was intact over these bands of localization indicating that the oxide followed the deformation of the underlying aluminide even though the local strains were large. There were, however, numerous cracks in the thermally grown oxide that emanated from these steps and had a tendency to propagate parallel to the applied stress direction as seen in Fig. 5 in some cases following grain boundaries on the oxide and crossing oxide grains elsewhere. From the variation in the crack opening with distance from the steps, it can be concluded that the cracks probably originated in the vicinity of the steps. Cross-sections of the cracks, obtained by focused ion beam (FIB), indicated that the cracks have a blunt tip, surrounded uniformly by oxide. This suggests that the crack blunts as a result of crack-tip plasticity during temperature and strain cycling. It is also noted that the aluminide deformation does not seem to be related to the deformation of the superalloy since the interface between the coating and the underlying superalloy, as well as the inter-diffusion zone, remains flat.

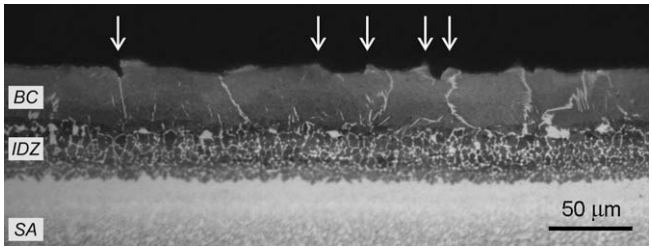

Fig. 4. Optical micrographs of the specimen cycled 82 times between 1000 and 1150 °C, cross-section along the load axis. The complex deformation is evident from the irregular nature of the gamma-prime precipitates (appearing light) in the coating (BC) and the steps and edges in the surface of the coating (arrowed). The inter-diffusion zone (IDZ) and underlying superalloy (SA) are labeled.

Author's personal copy

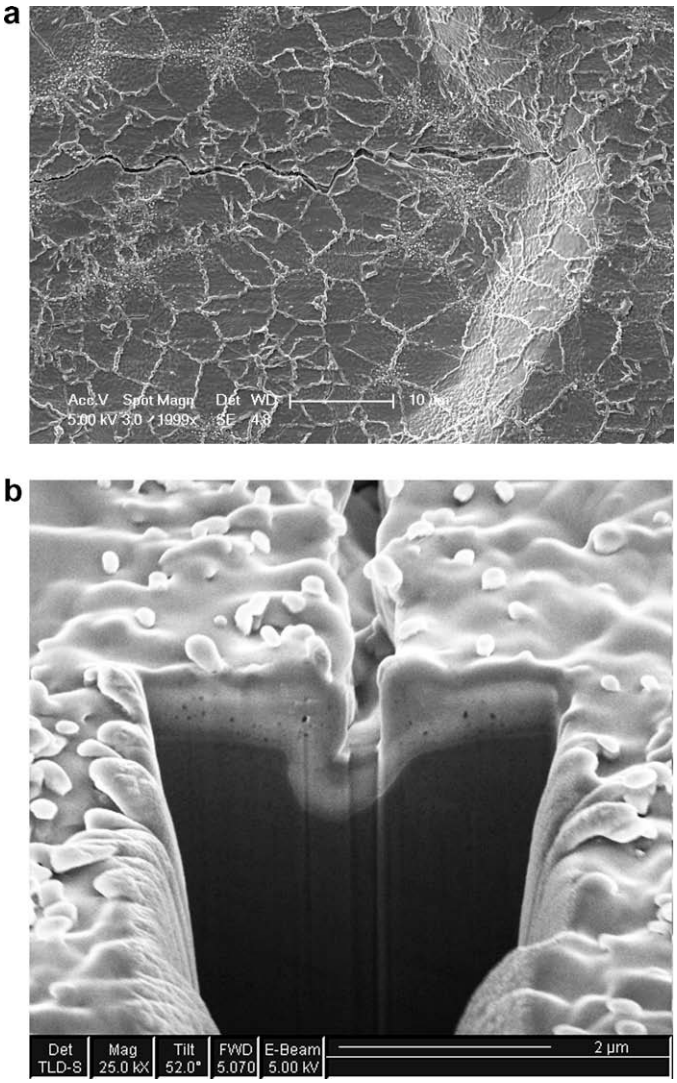

Fig. 5. (a) Higher magnification view of one of the abrupt steps produced perpendicular to the stress axis together with cracks in the thermally grown oxide. The cracks were not formed in the reference sample subjected to the same thermal cycling but absent applied stress. (b) FIB section through the crack.

4. Discussion

The observations in Fig. 2 clearly show that the applied compressive stress produces an alignment of the rumpling pattern perpendicular to the applied stress direction and that the alignment becomes both more pronounced and increases in amplitude with the number of thermal cycles. The quantitative analysis of the rumpling amplitude confirms that the roughness becomes progressively more asymmetric with continued cycling and increases linearly with the number of cycles. The second, and unexpected finding, is the occurrence of cracks in the thermally grown oxide and their alignment parallel to the applied stress direction. In the absence of an applied stress there is neither any preferred orientation of the rumpling pattern nor any cracks formed in the TGO.

Qualitatively, the alignment of the rumpling perpendicular to the applied compressive stress can be understood in terms of the buckling-ratcheting concept [10] of rumpling in which the surface rumpling is modeled as a surface morphology created by a mechanical buckling process. As has been established previously, the oxidation of the aluminide is accompanied by an in-plane growth strain associated with the oxidation molar volume change and so is under a biaxial compressive stress. If the oxide were not attached to the aluminide but constrained at the ends of the coating, it could lower its elastic strain energy by buckling but this is constrained by the underlying aluminide. At the temperatures involved, plastic deformation (including creep) of the aluminide can accommodate the local out-of-plane displacements necessary for buckling to occur and although this can occur under isothermal oxidation, much larger displacements occur under thermal cycling conditions [11]. This is attributed to cyclic plasticity since this is generally a more effective means of mass transport than creep alone. The rate of buckling then depends in a complicated way on the thermal expansion mismatch strains, the yield behavior of the aluminide and the oxide as a function of temperature as well as the thickening rate of the growing oxide, codified in the Balint-Hutchinson continuum mechanics model of rumpling [10]. Without an applied stress, the rumpling pattern is random with no preferred orientation since the stress in the oxide is biaxial and the deformation is controlled by the mean stress in the aluminide. However, just as a superimposed uniaxial stress in mechanical systems favors buckling in the direction of the stress by reducing the critical buckling condition, it is assumed that the applied compressive stress biases the stress in the TGO and favors alignment of the rumples perpendicular to the stress direction. The thermal expansion mismatch between the superalloy and bond-coat on thermal cycling provides the strain that motivates the plasticity in the aluminide and TGO.

The observed increase in directional anisotropy of the rumpling amplitude with the average rumpling amplitude shown in Fig. 3, suggests that the rumpling variants perpendicular to the applied stress grow at the expense those parallel to the stress direction. In turn, this implies that the overall strain energy reduction per cycle accompanying rumpling under a constant applied stress is fixed and that the plastic deformation accommodating the rumpling shape change is controlled by the mean stress in the aluminide rather than any specific component of the stress field. Furthermore, the differences in surface morphology, at different locations but on the same deformed specimen, suggest that the rumpling is dependent on the mean strain in the aluminide rather than the stress.

It is emphasized that although the applied stress was maintained constant during thermal cycling, the actual strain in the aluminide coating undergoes periodic cycling as a consequence of the difference in the thermal expansion coefficients between the superalloy and the coating. The thermal expansion coefficient of the aluminide coating we

Author's personal copy

have studied is not known but it is likely that it is similar to that of the single crystal NiAl shown in Fig. 6, drawn from the work of Haynes et al. [8]. An unusual feature of data is that although the thermal expansion of the NiAl varies almost linearly with temperature, the thermal expansion of the N5, as well as other second generation superalloys, such as the CMSX-4 used in this work, increases nonlinearly at temperatures above about 800 °C. Furthermore, there is a cross-over at around 850 °C of the two curves. The lower temperature of the thermal cycling used in this study, 1000 °C, was chosen in part because it is above this cross-over temperature and in part because the rumpling amplitude has been found to be maximal when the lower temperature in the cycling lies above 1000 °C [7]. Consequentially, over our thermal cycling regime, the thermal expansion coefficient of the superalloy is always larger than that of the aluminide except on final cooling thereby maximizing the magnitude of the mean strain in the aluminide per cycle.

At the microstructural level, the rumpling is associated with the relative displacement of the surfaces of individual grains with respect to the average surface plane. (The interferometer is sensitive to relative height over the scanned area). Detailed comparison of individual grains in the as-aluminized surface (Fig. 2d) with the image of the identical region after thermal cycling (Fig. 2b), indicates that the rumpling alignment is associated with the large grains swelling up relative to smaller grains shrinking down and that there is a spatial correlation in bands perpendicular to the applied stress direction. Thus, the bands are not continuous at the microstructural level but consist of individual grains, some staggered along the average alignment direction, whose outer surfaces have swollen up separated by grains whose surfaces have moved down. There is no apparent crystallographic dependence of the individual grains on their surface behavior. Previous studies of rumpling without any applied stress indicate that the rumples form as the center of grains with five and fewer sides shrink relative to the swelling of surface of grains with six or more sides [12]. This appears to be the case in these samples too but was not quantified in the same detail as in Ref. [12].

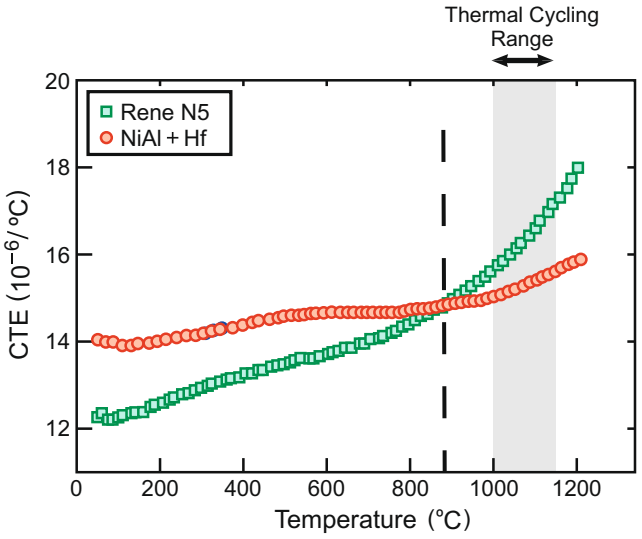

Fig. 6. The thermal expansion coefficient versus temperature for a single crystal NiAl alloy and single crystal superalloy Rene5, an alloy similar to the CMSX-4 alloy used in this work. The thermal cycling range is shown shaded. Data drawn from Haynes et al. [8].

The appearance of large steps and abrupt changes in the surface, as illustrated by both the interferometry images and the micrographs, in the portions of the specimen subject to the largest creep strain indicate extensive flow and localization of material perpendicular to the applied stress. In some places, sharp grooves and ridges are formed at the grain boundaries suggesting that flow is partially localized at these perpendicular zones. The occurrence of cracks in the thermally grown oxide, such as shown in Fig. 5, appears to be correlated with the formation of these localization features and, as mentioned earlier, no cracks were observed in the unstressed reference samples suggesting that their formation is related to the combination of the applied and thermal expansion mismatch stress. The fact that they are associated with the steps suggests a complex local and global deformation state but their general alignment parallel to the applied compressive stress and their opening is consistent with the expected strains in the aluminide and the oxide. The constant applied compressive stress creates through the Poisson effect an approximately constant tensile strain in the oxide and aluminide perpendicular to the applied loading direction. This is superimposed on the local strain concentrations plus the cyclic thermal strains that vary from zero at the maximum temperature, assuming relaxation of the stresses in the aluminide can occur at this temperature, and a maximum compression at the lower temperatures. So, in addition to the temperature varying compressive axial strain in the aluminide, once the superalloy deforms inelastically there is a tensile strain perpendicular to the applied load that can apply a permanent crack opening displacement on any incipient cracks nucleated at the sharp steps formed by the strain localization.

Acknowledgement

This work was supported by the Office of Naval Research under Contract A00014-04-1-0053. The authors are grateful to Dr. Ken Murphy, Howmet Research Corporation for supplying the materials studied in this work.

References

[1] Coatings for high temperature structural materials: trends and opportunities. Washington: National Research Council; 1996.
[2] Birks N, Meier GH, Pettit FS. Introduction to the high-temperature oxidation of metals. 2nd ed. Cambridge: Cambridge University Press; 2006.
[3] Reed RC. The superalloys: fundamentals and applications. Cambridge: Cambridge University Press; 2006.
[4] Tolpygo VK, Clarke DR. Temperature and cycle time dependence of rumpling in platinum-modified diffusion aluminide coatings. Scripta Mater 2007;57:563–6.

Author's personal copy

[5] Evans AG et al. The mechanism governing sustained peak low cyclic fatigue of coated superalloys. Acta Materialia, submitted for publication.
[6] Onofrio G, Osinkolu GA, Marchionni M. Fatigue crack growth of UDIMET 720 Li superalloy at elevated temperature. Int J Fatigue 2001;23:887–95.
[7] Tolpygo VK, Clarke DR. Effect of intermediate temperature thermal cycling on rumpling. Scripta Mater 2007.
[8] Haynes JA et al. Comparison of thermal expansion and oxidation behavior of various high-temperature coating materials and superalloys. Mater High Temp 2004;21(2):87–94.
[9] Raffaitin A et al. The effect of thermal cycling on the high temperature creep behavior of a single crystal nickel-based superalloy. Scripta Mater 2007;56:277–80.
[10] Balint DS, Hutchinson JW. An analytical model of rumpling in thermal barrier coatings. J Mech Physics Solids 2005;53(4):949–73.
[11] He MY, Evans AG, Hutchinson JW. The ratcheting of compressed thermally grown thin films on ductile substrates. Acta Mater 2000;48(10):2593–601.
[12] Dryepondt S, Porter JR, Clarke DR. Initiation of cyclic oxidation induced rumpling of platinum-modified nickel aluminide coatings. Acta Mater 2009; 57: 1717–23.